



Heat recovery of dedusting systems in electric arc furnaces: concept of a bottoming cogeneration plant and techno-economic analysis

Cesar Augusto Arezo e Silva Jr.¹ · José Alexandre Matelli¹

Received: 8 September 2017 / Accepted: 6 November 2017 / Published online: 30 December 2017
 © The Brazilian Society of Mechanical Sciences and Engineering 2017

Abstract

Steelworks require large amount of energy in reduction, fusion and refining processes. A mini-mill is a steelwork that produces steel by melting scrap metal, pig iron and metallic elements in electric arc furnaces. Depending on the desired product, the refining process requires vacuum degassing to remove contaminant gases from the liquid steel. The vacuum in the degassing process can be obtained through steam ejectors, which use superheated steam. Furthermore, environmental legislation requires mini-mills to have dedusting systems over the electric furnaces. In general, a dedusting system generates high flow rates of hot off-gases, which indicates an interesting potential for heat recovering. In this paper, a cogeneration plant to recover heat from the dedusting system of a Brazilian mini-mill is proposed. The actual operation data are considered to calculate the heat available and to conceptualize a bottoming cogeneration plant that generates electric power and superheated steam for the ejectors of the degassing process. Results show that the proposed plant can generate 45.4% of the steam required by the ejectors and up to 2.4% of the power required by the electric arc furnace. Also, the heat recovering from the dedusting system reduces the use of cooling water by 29.3%. From an economic viewpoint, the cogeneration plant decreased the expenses for power, steam and cooling water by 1.5, 32 and 29%, respectively. Overall, there was an expense reduction of 4.8%, resulting in a payback period of 4.1 years in the case base. For a projected best case scenario, the payback period is about 2.3 years.

Keywords Mini-mill · Electric arc furnace · Heat recovery · Cogeneration

Nomenclature

List of symbols

b_p	Bypass ratio [–]
C	Specific cost [USD/MWh]
c_p	Specific heat [kJ/kgK]
D_t	Tube diameter [m]
E	Expense [USD/year]
f	Annuity factor [–]
H	Annual operating time [h]
h	Specific enthalpy [kJ/kg]

I	Investment cost [USD]
j	Annual interest rate [–]
k	Plant useful life [years]
L	Length [m]
m	Mass [kg]
\dot{m}	Mass flow [kg/s]
N_t	Number of tubes [–]
P	Pressure [kPa]
pb	Payback [year]
q	Heat transfer rate [kW]
R	Revenue [USD/year]
r_{ev}	Evaporation rate [–]
s	Specific entropy [kJ/kgK]
T	Temperature [°C]
t	Time [s]
\dot{W}	Work transfer rate, power [kW]

Technical Editor: Jose A. dos Reis Parise.

✉ José Alexandre Matelli
 matelli@feg.unesp.br

Cesar Augusto Arezo e Silva Jr.
 cesar.arezo@hotmail.com

¹ School of Engineering, Department of Energy, São Paulo State University (UNESP), Guaratinguetá, SP, Brazil

Greek letters

Δ	Difference
η	Efficiency [–]
ρ	Specific mass [kg/m]

Subscripts

ap	Approach point
b	Gas-fired boiler
c	Colder than average condenser
cl	Cycle
cur	Current situation
cw	Cooling water
d	Degassing process
e	Electric energy
ec	Economizer section
ev	Evaporator section
g	Off-gas power generator
h	Hotter than average
he	Heat exchanger
i	Inlet
<i>i,j,k</i>	Indexes, counting variables
l	Loss
ng	Natural gas
o	Outlet
om	Operation and maintenance
p	Pump
pp	Pinch point
sat	Saturation
sg	(heat recovery) Steam generator
sh	Superheater section
sl	Salt
st	Steam
t	Turbine
tr	Thermal reservoir

Superscripts

cg	Cogeneration
off	Ejector off
on	Ejector on [–]

Abbreviations

ABNT	Brazilian Association of Tech. Standards
EAF	Electric arc furnace
HRSG	Heat recovering steam generator
LHV	Lower heating value
NBR	Brazilian standard
O&M	Operation and maintenance
TR	Thermal reservoir

1 Introduction

Rational use of energy is a major priority in Brazilian industry since the energy rationing in 2001. Just recently, hydro power plants' reservoirs were nearly empty, demanding the use of pollutant and expensive thermal power plants for long periods of time. Furthermore, global competition keeps demanding the reduction of production cost. Depending on the industrial sector, energy cost is a

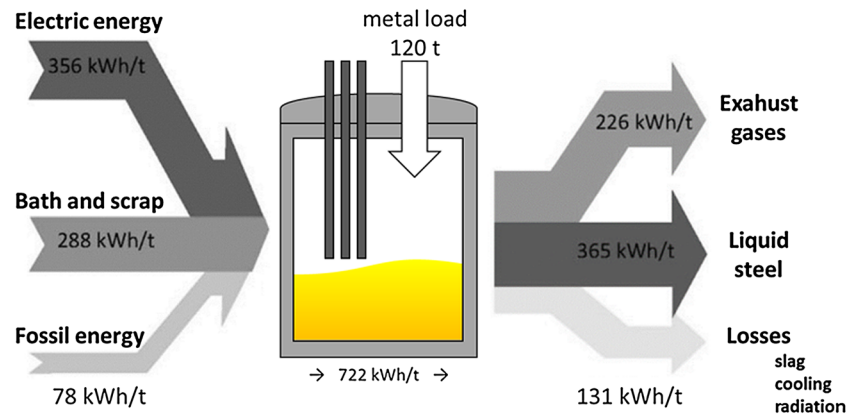
significant share of total production costs. In steelworks, this share is about 20%. In integrated steel mills, up to 75% of energy demand comes from fossil fuels and 64% of the total energy demand of a mini-mill is electric energy [1].

The main characteristics of a mini-mill are the use of metal scrap and pig iron as raw materials and the highly intensive use of electric power in melting and refining processes. Liquid steel is obtained in electric arc furnaces (EAF), where electric energy is converted to heat. The heat is then transferred to the metal load inside the furnace, where a temperature as high as 1600 °C is reached for load melting. Electric energy to melt the metallic load is about 50% of the total energy required in the EAF; 40% is provided by exothermic reactions within the furnace; and 10% is due to natural gas combustion and coal addition to the metallic bath [2]. The amount of energy that effectively melts the load is about 1314 kJ/kg (365 kWh/t) and the heat loss with the off-gases is about 813.6 kJ/kg (226 kWh/t), which is close to 30% of the total furnace energy input [2]. A typical energy balance of an EAF is shown in Fig. 1.

Large amounts of particulate matter are generated during the steel melting. To avoid releasing these pollutants into the atmosphere, a dedusting system is required. This system presents high flow rate of hot gases with high concentration of particulate matter and carbon monoxide from the furnace. The carbon monoxide is burned in a combustion chamber and the particulate matter is filtered in a baghouse. To prevent fire, the gas stream must be cooled down upstream the baghouse. Thus, the heat contained in this stream is lost. Contaminant gases are also present in the liquid metal and, depending on the desired product, a degassing process may be required to remove these gases through vacuum generated by steam ejectors.

Most of the Brazilian mini-mills do not recover heat from dedusting systems, so that there is significant potential to increase the energy efficiency of the overall mini-mill process. Recent publications present studies of heat recovery opportunities in steel mills, most of them referring to integrated steel mills [3–7]. Heat recovery for power generation in mini-mills is found in the works of Pili et al. [8], Ramirez et al. [9] and Nardin et al. [10]. None of these studies on heat recovery in steel mills (either integrated or mini) proposes the cogeneration of power and steam for industrial process, so that there is opportunity for an original contribution. The objective of this paper is to propose a bottoming cogeneration plant to recover heat from the dedusting system of a Brazilian mini-mill. Although it may be argued that the primary energy source is electric energy instead of heat from a burning fuel, in this work the term cogeneration is preferred in the sense that two utilities are simultaneously generated from heat recovery. The actual operation data are considered to calculate the heat available and to conceptualize a cogeneration plant that generates

Fig. 1 Sankey diagram for a typical EAF (adapted from [2])



power and superheated steam for the ejectors of the degassing process. The use of a thermal reservoir to damp the influence of furnace transient operation (batch operation) on the cogeneration plant is also evaluated.

2 Mini-mill description

The mini-mill considered in this work is located in São Paulo State, Brazil. The nominal capacity of EAF is 90 tons of steel per batch, with 45 MVA of electric power. The EAF is able to process a whole batch in about 100 min. Normally, the EAF is not loaded at once, but rather divided into intermediate loads. In the first loading, the metal scrap fills the entire furnace volume. When melted, however, the liquid metallic mass occupies a much smaller volume, resulting in more room in the furnace for subsequent loadings. The EAF considered in this work can operate with three intermediate loads to complete its total capacity. After the whole batch is melted, the liquid steel is transferred to a ladle furnace for subsequent refining.

During the EAF operation, it remains closed to avoid the release of heat and potentially hazardous off-gases with significant amounts of carbon monoxide and particulate matter. Because of that, the resulting off-gases are sent to a combustion chamber for burning. Then, the resulting gases are cooled down to be safely filtered in the baghouse. This path is called primary line (Fig. 2). When the melting is done, the EAF is opened. That opening releases gases in the industrial shed where the furnace is installed. The shed has a canopy in the ceiling to aspire the gases through the secondary line. In both lines, the gases are driven by fans. Since a large amount of ambient air is aspirated along with the gases in the canopy, the gases in the secondary line are much cooler, so that no further cooling is required upstream the baghouse. Primary and secondary lines and respective hardware are called dedusting system and is quite similar to that presented by Nardin et al. [10]. The mini-mill dedusting system is depicted in Fig. 2.

After slag removal, the liquid steel is transferred to a ladle for addition of chemicals to adjust the properties and equalization of steel temperature for subsequent conformation. Depending on the obtained steel, the vacuum degassing process is necessary before temperature equalization [11]. In this case, the ladle is put into a hermetically sealed vacuum furnace. The vacuum is obtained through steam ejectors that require up to 5.56 kg/s (20 t/h) of superheated steam at 1.50 MPa and temperature no less than 200 °C. Degassing is also a batch process; each batch lasts about 60 min, during which the steam demand is equal to 20 t/h for 30 min. For another 30 min, there is no demand. Currently, the superheated steam is provided by two natural gas-fired, water-tube steam generators, each with a rated capacity of 5.56 kg/s (20 t/h) at 2.2 MPa. The boilers also provide 1.67 kg/s (6 t/h) of steam at 1.2 MPa to another industrial process (Fig. 3).

The actual data from the data acquisition and controlling system of the mini-mill are considered in this work. Flow and temperature measures are taken in the primary line (Fig. 2) downstream the combustion chamber. Around 500,000 samples were collected during 40 days, which allowed to capture several different operational conditions for different steels produced in the EAF. Since off-gas flow is induced by the fan, the flow rate is equal to 253,500 Nm³/h, which is the nominal flow of the fan. Also, the flow rate is observed to be independent of the batch. Off-gas specific heat and specific mass are equal to 1.33 kJ/Nm³K and 1.3 kg/Nm³, respectively [10]. Off-gas temperature, on the other hand, presents significant variation. Table 1 presents consolidated data from 13 batches and 10 different products.

The instruments used to collect temperature data present errors of ± 1.5 °C. They are calibrated according to technical procedures specified in Brazilian standards issued by ABNT, such as NBR 13,863 and NBR 14,670. There is an instrumentation and control department responsible for the maintenance and calibration of all the measuring instruments and transducers used in the steelworks. The

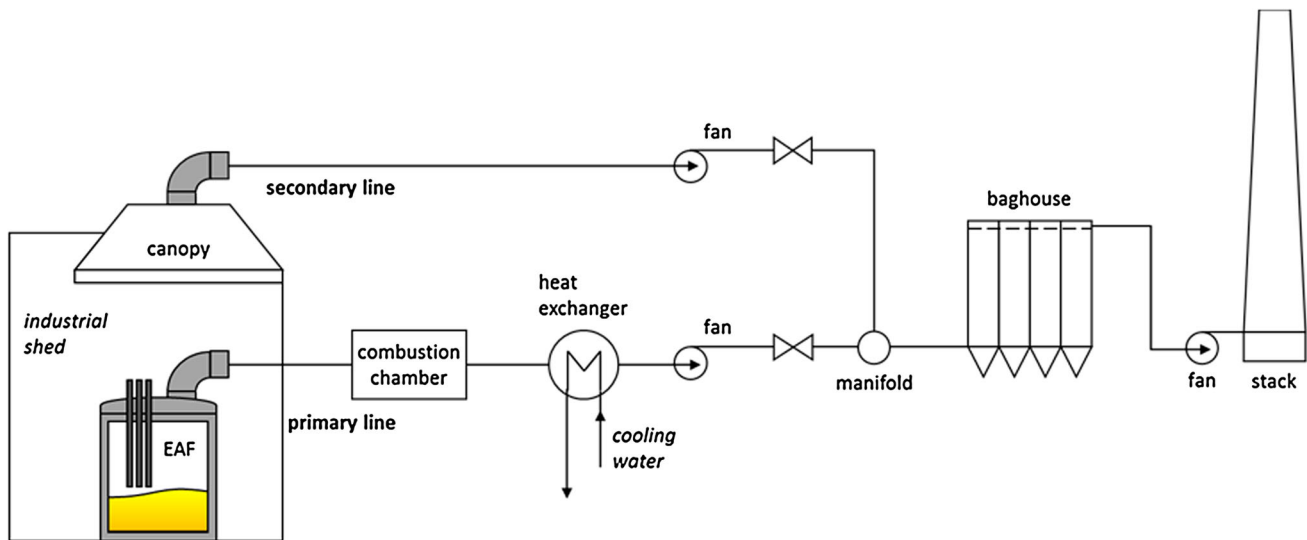
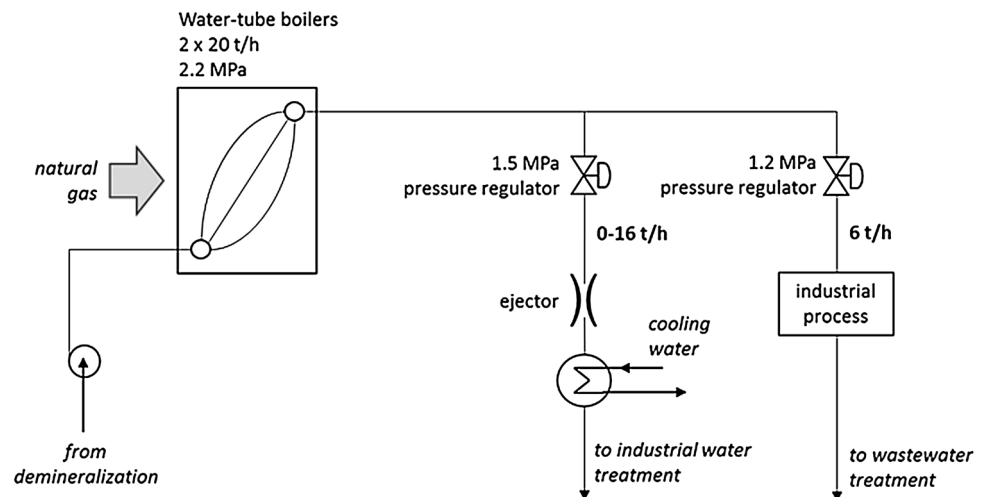


Fig. 2 Mini-mill dedusting system (adapted from [10])

Fig. 3 Steam generation for degassing and other industrial processes



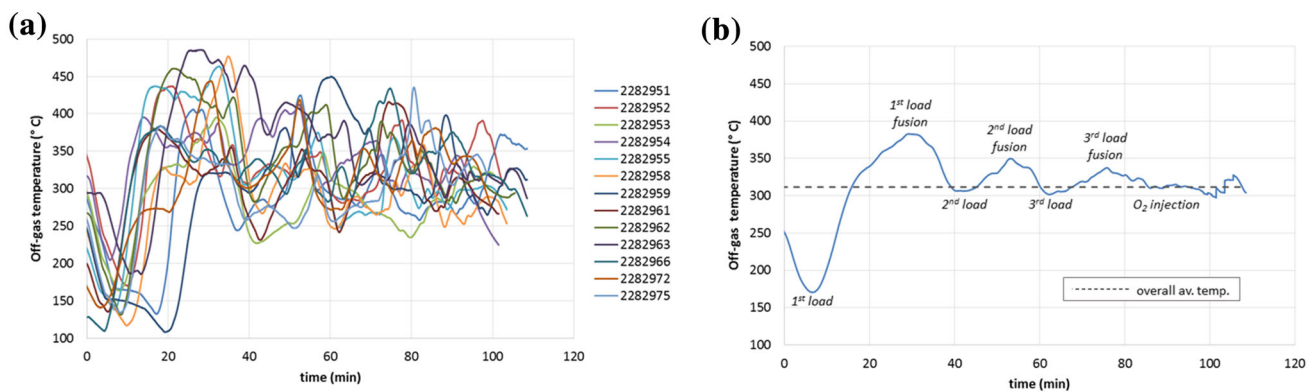
department has an accredited laboratory where calibrations are performed according a pre-defined schedule to assure a calibration confidence interval greater than 95%.

Figure 4 shows the off-gas temperature profile for each batch and the resulting off-gas average temperature profile. It is interesting to note that the average profile allows to identify when the intermediate loadings and respective melting occur. It also should be emphasized that the actual operational performance of the plant would depend on the batch being processed, so that the average profile is a parameter to make design decisions and not a way to predict the plant performance. From data analysis of Fig. 4b, the overall average temperature is equal to 311.8 °C and the off-gas presents temperature below the overall average for 2531 s (42.2 min). During this interval, the off-gas average temperature is about 273.8 °C. Not surprisingly, the first load contributes the most to the

interval on which off-gas temperature is lower than the average. This is an important design parameter for the cogeneration plant, since the plant is sized considering a heat source at the overall average temperature of 311.8 °C. During 42.2 min, the gases would not have enough energy to drive the plant. On the other hand, when the gases have temperature above the average, there would be more energy than the plant needs. Off-gas temperature exceeds the overall average during 3979 s (66.3 min) and, in this interval, the average off-gas temperature is about 336.1 °C. Thus, a thermal reservoir should be considered: (i) to store heat from the gases when exceeding heat is available during 66.3 min and (ii) to provide heat to the plant during 42.2 min when the gases have less energy than required. The detailed conception and modeling of the cogeneration plant and the heat reservoir are presented next in Sect. 3.

Table 1 Consolidated data from 13 batches in the EAF

Batch#	EAF operation time (min)			Off-gas av. temperature (°C)	Energy consumed (GJ)	Mass of steel produced (t)	Specific energy (GJ/t)	Steel type
	On, unloaded	On, loaded	Off, unloaded					
2282951	84	112	28	288.4	129	94.5	1.366	5140HM
2282952	82	103	21	324.8	133	95.5	1.391	9322A
2282953	82	101	19	285.7	136	95.5	1.423	9325A
2282954	75	102	27	333.9	124	93.9	1.323	1540HQ
2282955	78	104	26	319.0	129	93.7	1.374	1548HA
2282958	82	104	22	287.9	131	92.3	1.420	VC9
2282959	80	109	29	291.7	129	95.3	1.349	1548HA
2282961	83	102	19	304.4	131	91.4	1.434	15B35HD
2282962	83	106	23	333.6	132	95.3	1.383	1548HA
2282963	83	109	26	351.3	130	97.0	1.340	5120HB
2282966	85	109	24	320.8	142	97.7	1.455	5135HA
2282972	84	100	16	310.6	135	94.7	1.422	15V15HF
2282975	76	99	23	296.9	124	94.8	1.308	1548HA
Average	81.3	104.6	23.3	311.8	131	94.7	1.383	—

**Fig. 4** Off-gas temperature profile: **a** for each batch; **b** average profile

3 Methodology

3.1 Cogeneration plant conceptualization

The concept of the bottoming cogeneration plant is to recover the heat of the dedusting system to generate superheated steam to drive a condensation turbine and to feed the ejectors of the degassing system, as shown in Fig. 5. Heat recovery should take place in the primary line of the dedusting system, between the combustion chamber and the heat exchanger. The off-gas temperature is measured here, and is the highest at this place. A thermal reservoir (TR) is placed right after the combustion chamber in order to damp the EAF transient operation evinced in Fig. 4. When the off-gas temperature exceeds the TR temperature, the gas stream transfers heat to the reservoir;

otherwise, TR transfers heat to the gas stream. After leaving the TR, the off-gas enters a heat recovery steam generator (HRSG), where superheated steam is generated. To keep the mini-mill operation flexible, the cogeneration plant should operate in parallel with the existing natural gas-fired boilers. Furthermore, if the cogeneration plant needs to be shut down for any reason, TR and HRSG can be bypassed to keep the mini-mill working. In this situation, the gas-fired boilers should meet the steam demand. The design parameters adopted for the cogeneration plant are shown in Table 2.

Regarding the thermal reservoir design, it is considered to be built with stainless steel tubes filled with a mixture of 60% NaNO_3 (mass basis) and 40% KNO_3 . In this proportion, the salt mixture melts at 220 °C, remains in two-phase (solid–liquid) state up to 240 °C and boils at 550 °C. It

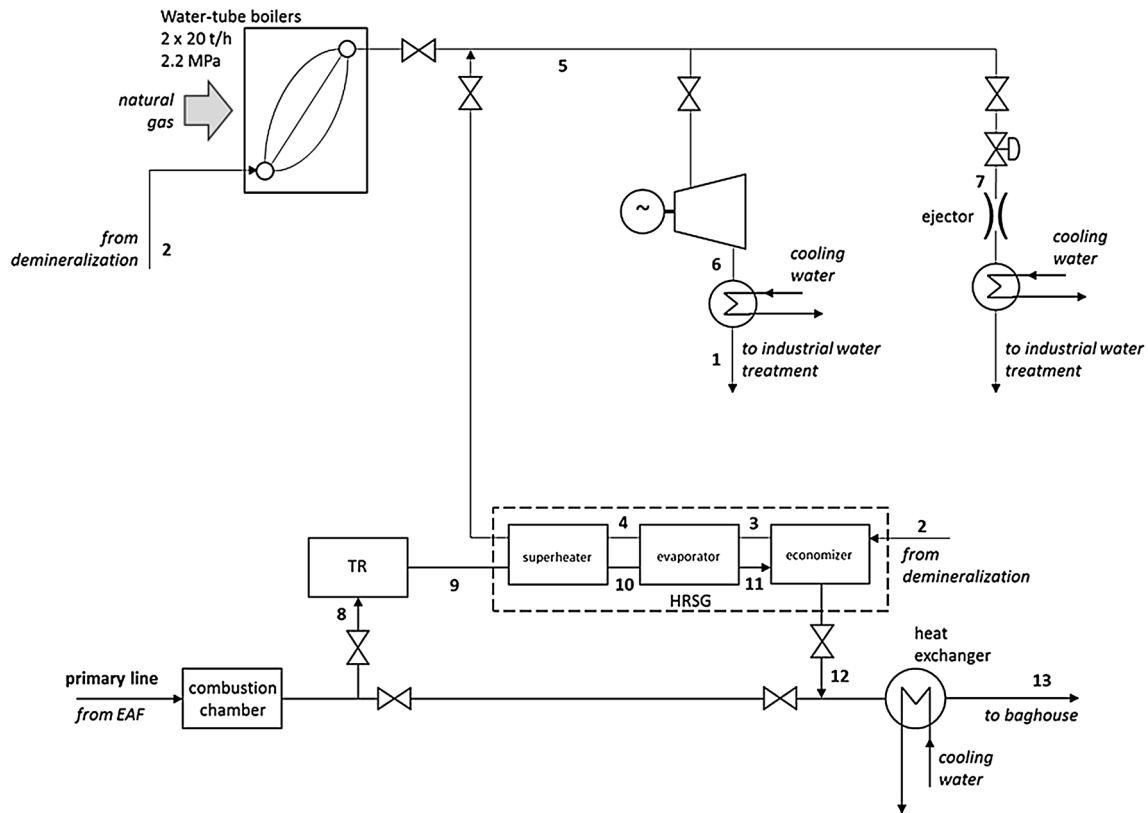


Fig. 5 Concept of the bottoming cogeneration plant

Table 2 Design parameters of the cogeneration plant

Point (Fig. 5)	Description	Adopted values	Note
1	Condenser outlet	$P_1 = 50 \text{ kPa}$; $T_1 = 45 \text{ }^\circ\text{C}$	To approximately match the demineralized water state
5	Turbine inlet	$P_5 = 2.2 \text{ MPa}$; $T_5 = 300 \text{ }^\circ\text{C}$	To match the existing boiler pressure
6	Turbine outlet	$P_6 = 50 \text{ kPa}$	Typically adopted to assure a proper turbine operation
7	Ejector inlet	$P_7 = 1.5 \text{ MPa}$	Actual process requirement, mass flow up to 20 t/h
8	TR off-gas inlet	$\dot{m}_8 = \dot{m}_g = 91.54 \text{ kg/s}$	Actual off-gas flow
9	HRSG off-gas inlet	$T_9 = 311.8 \text{ }^\circ\text{C}$	Average off-gas temperature (see Sect. 2)
12	HRSG off-gas outlet	$T_{12} \geq 130 \text{ }^\circ\text{C}$	To avoid acid condensation
13	Baghouse off-gas inlet	$T_{13} \leq 130 \text{ }^\circ\text{C}$	To avoid fire in the baghouse

presents specific heat equal to 1.5 kJ/kgK and specific mass equal to 1800 kg/m^3 [13]. The TR preliminary design resembles a shell-and-tube heat exchanger without baffles, with the off-gas flowing parallel to the tube's orientation, as shown in Fig. 6. The length of 25 m is chosen to fit the available space in the mini-mill. The mass of salt mixture within the TR tubes should be enough to keep the salt mixture completely liquid during the EAF operation.

3.2 Thermal reservoir design

A lumped thermodynamic model is proposed to calculate the required mass of salt in the TR and its temporal

temperature profile. This model is justified because the TR geometry is not fully defined during the basic thermal design, so that it is not possible to take into account heat transfer coefficients that are dependent on the geometry. For the thermodynamic model, it is considered that:

- TR is adiabatic and damps the off-gas transient temperature to the average value, so that the off-gas temperature in the TR outlet (point 9 in Fig. 5) is $T_9 = 311.8 \text{ }^\circ\text{C}$;
- During the lumped period Δt_h on which the off-gas are hotter than the salt, the average temperature in the TR inlet (point 8 in Fig. 5) is $\bar{T}_{8,h} = 336.1 \text{ }^\circ\text{C}$;

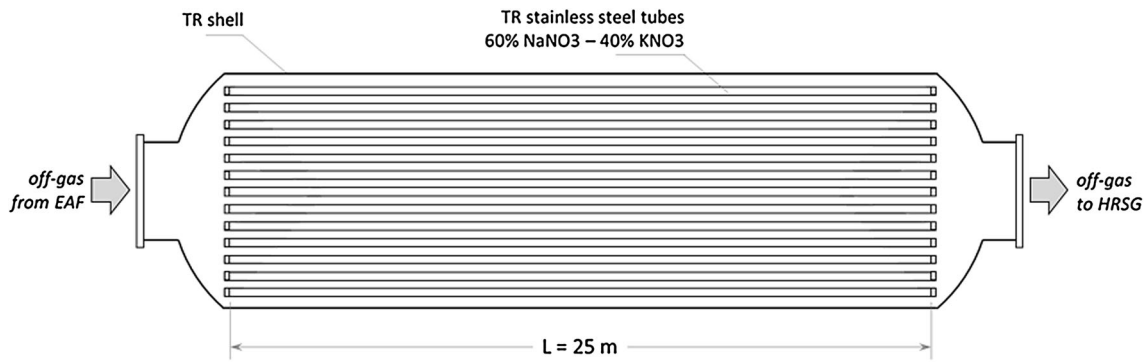


Fig. 6 Thermal reservoir design

- iii. During the period Δt_c on which the off-gas are colder than the salt, the average temperature in the TR inlet is $\bar{T}_{8,c} = 273.8^\circ\text{C}$;
- iv. The salt temperature varies between $T_{s,\min} = T_9$ and $T_{s,\max} = \bar{T}_{8,h}$, and also the salt properties are constant.

During period Δt_h , the off-gas enters the TR with temperature $\bar{T}_{8,h}$ and leaves it with temperature T_9 , resulting in a heat transfer rate calculated according to Eq. 1, on which $\dot{m}_g = \dot{m}_8 = \dot{m}_9$,

$$q_{g,TR} = \dot{m}_g c_{p,g} (\bar{T}_{8,h} - T_9). \quad (1)$$

The off-gas heat is transferred to the salt, so that it requires the time interval Δt_h to increase the salt mass temperature from $T_{sl,\min}$ to $T_{sl,\max}$. Thus, the required mass is calculated according to Eq. 2:

$$m_{sl} = \frac{q_{g,TR} \Delta t_h}{c_{p,sl} (T_{sl,\max} - T_{sl,\min})} = \frac{\dot{m}_g c_{p,g} \Delta t_h}{c_{p,sl}}. \quad (2)$$

Of course, the mass of salt could be alternatively calculated for the period Δt_c on which the off-gas enters the TR with temperature $\bar{T}_{8,c}$. Knowing the mass of salt, the number of tubes required for the TR is calculated according to Eq. 3. From the mass salt and the actual off-gas temperature profile (Fig. 4), the salt temperature profile can be numerically determined by applying Eq. 4 to every instant t_k , assuming that at t_0 , $T_{sl,0} = T_{s,\max}$,

$$N_t = \frac{4m_{sl}}{\pi D_t^2 L \rho_{sl}}, \quad (3)$$

$$T_{sl,k} = T_{sl,k-1} + \frac{\dot{m}_g c_{p,g} [T_{8,k} - T_9]}{m_{sl} c_{p,sl}} (t_k - t_{k-1}). \quad (4)$$

3.3 Cogeneration design

Basically, the cogeneration plant is sized by applying mass and energy balances to each component of the plant (Eqs. 5–6, respectively), under the following hypothesis:

- i. There is steady state, since the TR damps the transient effects from the EAF;
- ii. The off-gas properties are constant;
- iii. The efficiencies are considered for HRSG, steam turbine, power generator and pump;
- iv. Any pressure drop and heat losses in pipes and valves are neglected;

$$\sum \dot{m}_i = \sum \dot{m}_o; \quad (5)$$

$$q - \dot{W} = \sum \dot{m}_o h_o - \sum \dot{m}_i h_i. \quad (6)$$

Application of Eqs. 5–6 to each component is detailed as follows.

3.3.1 HRSG

The HRSG is divided into three sections: superheater, evaporator and economizer. According to Lora and Nascimento [13], heat loss to ambient can be reduced up to 3% of the energy input. Based on this, an efficiency of $\eta_{sg} = 0.97$ in each section of this component is admitted. For the off-gas stream, Eq. 5 is $\dot{m}_g = \dot{m}_9 = \dot{m}_{10} = \dot{m}_{11} = \dot{m}_{12}$; for the steam one, it is $\dot{m}_{st} = \dot{m}_2 = \dot{m}_3 = \dot{m}_4 = \dot{m}_5$. Provided the pinch point ΔT_{pp} (Eq. 7), steam flow is calculated from an energy balance on the superheater (Eq. 8). A proper choice of the pinch point assures the best trade-off between heat recovery and off-gas temperature in the outlet.

$$\Delta T_{pp} = T_{10} - T_4 = T_9 - T_{sat}(P_5), \quad (7)$$

$$\dot{m}_{st} = \frac{\eta_{sg} \dot{m}_g c_{p,g} (T_9 - T_{10})}{h_5 - h_4}. \quad (8)$$

In a similar way, off-gas temperature leaving the evaporator is calculated from an energy balance (Eq. 9), provided the approach point ΔT_{ap} (Eq. 10). The approach point assures that no evaporation occurs in the economizer. Finally, the HRSG outlet temperature results from the energy balance on the economizer (Eq. 11).

$$T_{11} = T_{10} - \frac{\dot{m}_{st}(h_4 - h_3)}{\eta_{sg}\dot{m}_g c_{p,g}}, \quad (9)$$

$$\Delta T_{ap} = T_4 - T_3 = T_{sat}(P_5) - T_3, \quad (10)$$

$$T_{12} = T_{11} - \frac{\dot{m}_{st}(h_3 - h_2)}{\eta_{sg}\dot{m}_g c_{p,g}}. \quad (11)$$

3.3.2 Condensing turbine

The actual enthalpy in the turbine outlet is calculated from an isentropic efficiency $\eta_t = 0.7$ [14], as shown in Eq. 12. The power output is then calculated from the energy balance expressed in Eq. 13, taking into account the power generator efficiency $\eta_g = 0.95$.

$$h_6 = h_5 - \eta_t[h_3 - h(P_6, s_5)], \quad (12)$$

$$\dot{W}_e = \eta_g \dot{m}_{st}(h_5 - h_6). \quad (13)$$

3.3.3 Condenser

The thermodynamic state of the industrial water treatment is considered approximately the same as the steam leaving the condenser, so that the heat rejected on it is calculated as shown in Eq. 14. Knowing the difference of temperature of the cooling water ΔT_{cw} and adopting a specific heat constant for liquid water $c_{p,cw} = 4.182$ kJ/kgK, the cooling water flow in the condenser is calculated from Eq. 15.

$$q_c = \dot{m}_{st}(h_6 - h_1), \quad (14)$$

$$\dot{m}_{cw,c} = \frac{q_c}{c_{p,cw}\Delta T_{cw}}. \quad (15)$$

3.3.4 Pump

Similarly to the turbine, an isentropic pumping efficiency $\eta_p = 0.8$ [14] is considered to calculate the actual enthalpy in the pump outlet, as shown in Eq. 16. The required pumping power is calculated according to Eq. 17.

$$h_2 = h_1 + \frac{h(P_2, s_1) - h_1}{\eta_p}, \quad (16)$$

$$\dot{W}_p = \dot{m}_{st}(h_2 - h_1). \quad (17)$$

3.3.5 Heat exchanger

To be safely filtered in the baghouse, the off-gas temperature should not exceed $T_{13} = 130^\circ\text{C}$. Depending on the HRSG off-gas outlet temperature T_{12} , further cooling in the heat exchanger downstream the HRSG could be necessary.

Similarly to Eq. 13, the cooling water flow in the heat exchanger is calculated from an energy balance (Eq. 18):

$$\dot{m}_{cw,he} = \frac{\dot{m}_g c_{p,g}(T_{12} - T_{13})}{c_{p,cw}\Delta T_{cw}}. \quad (18)$$

3.4 Economic analysis

The economic analysis is based on equations for investment cost of the plant components found in Santos [15], except for the investment cost of the thermal reservoir, which is calculated based on premises adopted by Gaggioli et al. [12]. Equations for specific costs of electric energy and steam are adapted from Vilela [16]. The main economic parameters adopted are shown in Table 3.

The investment cost for steam turbine (with generator), HRSG, condenser and pump are given in Eqs. 19–22 [15], respectively. In these equations, the units for power is kW; for temperature $^\circ\text{C}$; for mass flow kg/s; and for enthalpy kJ/kg:

$$I_t = 59.495 \dot{W}_e^{0.70} \left[1 + \left(\frac{1 - 0.95}{1 - \eta_t} \right)^3 \right] \left[1 + 5 \left(\frac{T_5 - 86.6}{10.42} \right) \right], \quad (19)$$

$$I_{sg} = 4745 \left[\frac{h_5}{\log_{10}(T_9 - T_{12})} \right]^{0.8} + 11820 \dot{m}_{st} + 658 \dot{m}_g, \quad (20)$$

$$I_c = 1773 \dot{m}_{st}, \quad (21)$$

$$I_p = 4991.4 \dot{W}_p^{0.71} \left[1 + \left(\frac{1 - 0.80}{1 - \eta_p} \right)^3 \right]. \quad (22)$$

The investment cost of the thermal reservoir is calculated considering unitary costs (USD/kg_{sl}) adapted from Gaggioli et al. [12], except for the tubes cost, which is adjusted with actual market prices. The detailed costs of the TR are shown in Table 4, resulting then in Eq. 23:

$$I_{tr} = 5.63 m_{sl} + 8583 N_t^{0.4997}. \quad (23)$$

The equations for specific costs of electric energy and steam found in Vilela [16] require an annuity factor f that takes into account the annual interest rate j (expressed as decimal, not percentage) and plant useful life k (in years), as shown in Eq. 24:

$$f = \frac{j(1+j)^k}{(1+j)^k - 1}. \quad (24)$$

Regarding the electric energy specific cost (USD/MWh), it depends on which steam stream drives the turbine. Here, the turbine is driven by the steam provided by the HRSG, so that the specific cost is given in Eq. 25 (adapted from

Table 3 Parameters adopted for economic analysis (1 USD = 3.40 BRL)

Description	Adopted value	Note
Electric energy cost (C_e)	59.12 USD/MWh	Actual value of the mini-mill in 2016
Cost of nat. gas (C_{ng})	0.28 USD/m ³	Actual value of the mini-mill in 2016
Cost of cooling water (C_{cw})	1.00 USD/m ³	Actual value of the mini-mill in 2016
Cogeneration O&M cost ($C_{om,cg}$)	15 USD/MWh	According to Vilela [16]
Existing boiler O&M cost ($C_{om,b}$)	5 USD/MWh	Actual value of the mini-mill in 2016
Annual operating time (H)	7920 h	According mini-mill maintenance schedule
Cogen. plant useful life (k)	15 years	Stipulated
Annual interest rate (j)	12%	Stipulated

Table 4 Detailed TR costs

Description	Adopted value	Note
Shell	1.32 USD/kg _{stl}	Adapted from [12]
Foundation	4.16 USD/kg _{stl}	Adapted from [12]
Insulation	0.15 USD/kg _{stl}	Adapted from [12]
Tubes	–	Last term of Eq. 19

[16]). In this equation, it is considered that the investments required are the turbine and the condenser. Also, units of power, annual operating time and O&M cost are MW, h and USD/MWh, respectively:

$$C_{e,cg} = \frac{f(I_t + I_c)}{H\dot{W}_e} + \frac{C_{om,cg}(I_t + I_c)}{\sum_i I_i}. \quad (25)$$

For the steam specific cost (USD/MWh) generated in the HRSG, it is considered that the investments required are the HRSG, pump and TR (Eq. 26, adapted from [16]). For the steam generated in the existing boilers, the specific cost is shown in Eq. 27. In this equation, the annuity factor and investments are not considered because the boilers are already amortized. Note that in Eqs. 25 and 26, the cogeneration O&M cost is split proportionally to the respective investments.

$$C_{st,sg} = \frac{f(I_{sg} + I_p + I_{tr})}{H\dot{m}_{st}(h_5 - h_2)} + \frac{C_{om,cg}(I_{sg} + I_p + I_{tr})}{\sum_i I_i}, \quad (26)$$

$$C_{st,b} = \frac{C_{ng}}{\eta_b LHV} + C_{om,b}. \quad (27)$$

The current annual expenses of the EAF and the ones of the EAF with cogeneration are calculated through Eq. 28. The respective expenses $E_{i,j}$ for this equation are shown in Table 5. It should be noted that the expenses with steam are considered over half of the annual operating time H , because the degassing process demands steam only approximately 30 min/h (see Sect. 2). A steam bypass ratio b_p is also taken into account for this expense and the reason for that is explained later in Sect. 4.2. The cooling water

expense is basically the cost of make-up water to compensate evaporation in the cooling tower, which is quantified through an evaporation ratio r_{ev} . The net annual revenue is the difference between the expenses (Eq. 29) that are used to calculate the payback period (Eq. 30).

$$E_i = \sum_j E_{i,j}, \quad (28)$$

$$R = E_{cur} - E_{cg}, \quad (29)$$

$$pb = \sum I/R. \quad (30)$$

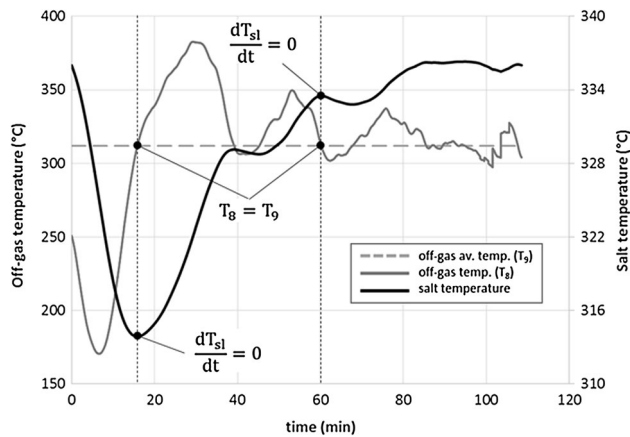
4 Results

4.1 Thermal reservoir

For the given off-gas temperature profile, the TR accumulates heat during 3978 s and releases heat during 2531 s to provide 91.536 kg/s of off-gas at 311.8 °C to the HRSG. Thus, the required mass of salt in the TR is 248,448 kg, which corresponds to a volume equal to 138 m³. This amount of salt results in a heat storage capacity of 9018.7 MJ. The maximum temperature of the salt is 336.3 °C at approximately 95 min of EAF operation; the minimum one is 313.9 °C at 16 min. The salt is stored into 77 stainless steel 12" tubes, schedule 40, each tube with 25 m length. This is a commercially available tube with internal diameter equal to 303.23 mm (11.938"). The temperature profile of the salt, along with the off-gas temperature profile, is shown in Fig. 7. It is interesting to note that when the TR transfers heat to the off-gas, $dT_{sl}/dt < 0$ for every instant on which $T_8 < T_9$. Conversely, when the TR stores heat from the off-gas, $dT_{sl}/dt > 0$ for every instant on which $T_8 > T_9$. On every instant when $T_8 = T_9$, the slope changes, i.e., $dT_{sl}/dt = 0$. That is quite clearly depicted in Fig. 7 for $t \cong 16$ min and $t \cong 60$ min. It can also be easily proved by rearranging Eq. 4 as Eq. 31: it is positive when $T_8 > T_9$, negative when $T_8 < T_9$ and zero for $T_8 = T_9$.

Table 5 Expenses with power, steam and cooling water in each situation

<i>j</i>	Expense	Current situation (<i>i</i> = cur)	With cogeneration (<i>i</i> = cg)	
			Ejectors off	Ejectors on
Power	$E_{i,p}$	$\dot{W}_{e, EAF} HC_e$	$\left(\dot{W}_{e, EAF} - \dot{W}_{e, cg}^{off} \right) \frac{H}{2} C_e + \dot{W}_{e, cg}^{off} \frac{H}{2} C_{e, cg}$	$\left(\dot{W}_{e, EAF} - \dot{W}_{e, cg}^{on} \right) \frac{H}{2} C_e + \dot{W}_{e, cg}^{on} \frac{H}{2} C_{e, cg}$
Steam	$E_{i, st}$	$\dot{m}_{st, d} (h_5 - h_2) \frac{H}{2} C_{st, b}$	—	$(h_5 - h_2) \frac{H}{2} \left[(\dot{m}_{st, d} - b_p \dot{m}_{st}) C_{st, b} + b_p \dot{m}_{st} C_{st, sg} \right]$
Cooling water	$E_{i, cw}$	$r_{ev} (\dot{m}_{cw, he} / \rho_w) HC_{cw}$	$r_{ev} \left[\left(\dot{m}_{cw, he}^{cg} + \dot{m}_{cw, c}^{off} \right) / \rho_w \right] \frac{H}{2} C_{cw}$	$r_{ev} \left[\left(\dot{m}_{cw, he}^{cg} + \dot{m}_{cw, c}^{on} \right) / \rho_w \right] \frac{H}{2} C_{cw}$

**Fig. 7** Temperature profile of the salt (TR)

$$\frac{dT_{sl}}{dt} = \lim_{\Delta t \rightarrow 0} \frac{\Delta T_{sl}}{\Delta t} = \frac{\dot{m}_g c_{p, g}}{\dot{m}_{sl} c_{p, sl}} (T_8 - T_9). \quad (31)$$

4.2 Cogeneration plant

The results for each point of the cogeneration plant depicted in Fig. 5 are shown in Table 6. The approach point is set to 10 °C and the pinch point is adjusted to 10 °C to result in an HRSG off-gas outlet temperature of $T_{12} = 199.8^\circ\text{C}$. The temperature profile of the HRSG is shown in Fig. 8. The other results are summarized as follows:

Heat recovered from off-gas in the HRSG: $q_g = 10491.5 \text{ kW}$.

Superheater: $q_{g, sh} = 806.9 \text{ kW}$.

Evaporator: $q_{g, ev} = 7106.3 \text{ kW}$.

Economizer: $q_{g, ec} = 2578.3 \text{ kW}$.

Heat transferred to generate steam in the HRSG: $q_{st} = 10176.8 \text{ kW}$.

Superheater: $q_{st, sh} = 782.7 \text{ kW}$.

Evaporator: $q_{st, ev} = 6893.2 \text{ kW}$.

Economizer: $q_{st, ec} = 2500.9 \text{ kW}$.

Heat loss in the HRSG: $q_l = 314.7 \text{ kW}$.

Steam flow produced by the HRSG: $\dot{m}_{st} = 3.600 \text{ kg/s}$.

Power generated in the turbine: $\dot{W}_e = 1634.1 \text{ kW}$.

Heat transferred in the condenser: $q_c = 8465.5 \text{ kW}$.

Power required by the pump: $\dot{W}_p = 8.867 \text{ kW}$.

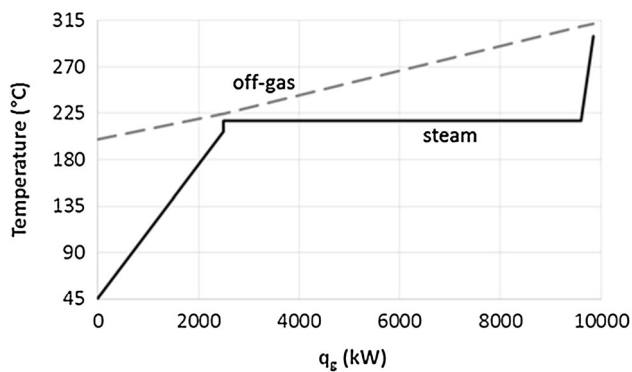
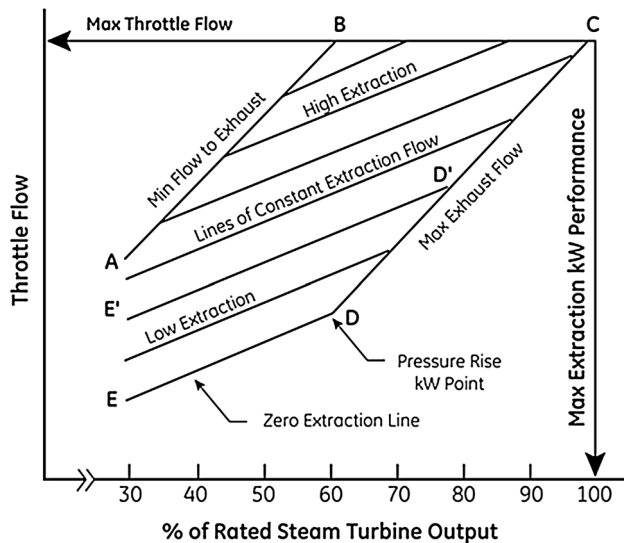
Cycle efficiency¹: $\eta_{cl} = 0.1549$.

The operation of the steam turbine, pump and condenser depends on the operation of the degassing process. During 30 min when there is no steam demand for degassing, the turbine operates at its rated capacity $\dot{W}_e = 1634.1 \text{ kW}$ and the condenser transfers $q_c = 8465.5 \text{ kW}$. During the other 30 min, the ejectors of the degassing process require steam, so that part of the steam generated in the HRSG is diverted from the turbine to the ejectors. However, a minimum steam flow should keep driving the turbine. Based on the condensing turbine typical performance map shown in Fig. 9 [17], the minimum flow in the steam turbine adopted in this work is 30% of the nominal flow, which results in a bypass ratio of $b_p = 0.7$. Thus, only 2.520 kg/s of steam generated in the HRSG can be diverted from the turbine to meet the degassing process ($\dot{m}_{st, d} = 5.556 \text{ kg/s}$); the difference of 3.036 kg/s should be provided by the existing boilers. The need for cooling water in both condenser and heat exchanger is calculated considering a typical difference of temperature $\Delta T_{cw} = 5^\circ\text{C}$. Cooling in the heat exchanger downstream the HRSG is necessary because the HRSG off-gas outlet temperature $T_{12} = 199.8^\circ\text{C}$ is still high to be safely filtered in the baghouse. Without the cogeneration plant, the water flow required in the heat exchanger is $\dot{m}_{cw, he} = 814.21 \text{ kg/s}$. It should be noted that the operation of TR, HRSG and heat exchanger does not depend on the degassing process operation. Table 7 summarizes the plant operation against the degassing process operation.

¹ $\eta_{cl} = (\dot{W}_e - \dot{W}_p) / q_g$.

Table 6 Results for each point of the cogeneration plant

Point (Fig. 5)	\dot{m} (kg/s)	T (°C)	P (kPa)	h (kJ/kg)	s (kJ/kgK)	X
1	3.600	45.0	50	188.47	0.6386	Comp. liq.
2	3.600	45.1	2200	190.93	0.6395	Comp. liq.
3	3.600	207.3	2200	885.58	2.399	Comp. liq.
4	3.600	217.3	2200	2800.2	6.304	1.000
5	3.600	300.0	2200	3017.6	6.717	Sup. steam
6	3.600	81.3	50	2538.8	7.295	0.954
7	Up to 5.556	286.8	1500	3017.6	6.868	Sup. steam
8	91.536	Variable	–	–	–	Off-gas
9	91.536	311.8	–	–	–	Off-gas
10	91.536	303.2	–	–	–	Off-gas
11	91.536	227.3	–	–	–	Off-gas
12	91.536	199.8	–	–	–	Off-gas
13	91.536	130.0	–	–	–	Off-gas

**Fig. 8** Temperature profile in the HRSG**Fig. 9** Typical turbine performance map [17]

4.3 Economic analysis

Investment costs required for the plant are shown in Table 8. Considering the data presented in Table 3, the cost of electric energy generated by the plant is 22.85 USD/MWh and the cost of the steam generated in the HRSG is 11.24 USD/MWh. The cost of the steam generated by the existing boilers is 36.17 USD/MWh. From these costs, it is possible to calculate the annual expenses of the current situation and the expenses with the cogeneration plant, as shown in Table 9.

From the total investment in Table 8 and the total revenue in Table 9, a payback period equal to 4.06 years is found. The results presented in Tables 8 and 9 are considered the base case for a sensibility analysis. A variation of + 10% is established in a given parameter of Table 3 (keeping the remaining ones unchanged) to calculate how much it affects the payback period. In addition to the parameters of Table 3, the bypass ratio and total investment are also considered in the sensibility analysis. The sensibility analysis results are shown in Table 10.

Results from Table 10 show quite clearly that the parameters that most affect the payback period are the total investment I , the number of operating hours H , the natural gas cost C_{ng} , the bypass ratio b_p , the electric energy cost C_e and the O&M costs for cogeneration $C_{om, cg}$, respectively. The TR has a huge impact on the total investment cost and shows quite clearly the influence of transient off-gas temperature on the economic attractiveness.

A range from – 20 to 20% variation on each of these parameters is established to investigate in more detail how each parameter influences the payback, as shown in Fig. 10. The bypass ratio has its maximum value at the base case and it cannot be further increased due to the technical reasons presented in Sect. 4.2. Because of that, it is not depicted in Fig. 10. The operating hours also are

Table 7 Plant operation against degassing process operation

Parameter	Degassing process operation	
	Ejectors off	Ejectors on
Steam flow (kg/s)		
Ejectors	0	5.556
HRSG	3.600	3.600
Turb./cond.	3.600	1.080
Boiler	0	3.036
Cooling water flow (kg/s)		
Condenser	404.85	121.46
Heat ex.	312.47	312.47
Turb. power output (kW)	1634.1	490.23
Pump power input (kW)	8.867	13.68
Plant net power output (kW)	1625.2	476.55
Cond. heat transfer (kW)	8465.5	2539.7
Nat. gas for the boiler ^a		
Heat (kW)	0	10,096.2
Flow (m ³ /h)	0	955.27

^aLHV 38,048 kJ/m³; $\eta_b = 0.85$

Table 8 Investment costs

<i>i</i>	Component	<i>I_i</i> (10 ⁶ USD)
1	Turbine (with generator)	1.087
2	HRSG	1.727
3	Condenser	0.006383
4	Pump	0.06396
5	Thermal reservoir	1.474
Total		4.358

limited to a maximum of + 5% variation because, otherwise, the EAF maintenance times would be fairly unrealistic. It is interesting to note that two of the most influential parameters (H and $C_{om, cg}$) are not subject, to some extent,

to external factors and depend only (again, to some extent) on the maintenance team of the mini-mill. If the maintenance team keeps up with the challenge to increase H by 5% and reduce $C_{om, cg}$ by 5%, the payback period would result in 3.78 years. Within the variation limits considered in Fig. 10, the worst scenario would result in a payback period equal to 9.98 years, as long as the most optimistic one would result in 2.31 years.

It is quite rare for Brazilian industries to accept investments with payback period higher than 3 years, so that the cogeneration plant proposed here is not attractive in the base case scenario for the mini-mill considered (it would be attractive in the best case scenario, though). The scale of the plant, irreversibilities and the need to cogenerate power to match the steam demand of the degassing system can be additional factors that affect the economic attractiveness, which must be further investigated. Alternatives that involve heat recovery only for steam generation should also be considered. Further economic and viability analysis should consider scenarios predicting a trend of increasing energy prices in Brazil and long-term energy supply contracts.

It is interesting to note that the payback is not that far from acceptance. As a matter of fact, the OECD Steel Committee [18] carried out a survey in the steel industry and identified long payback periods as one of the “issues facing companies that are otherwise interested in investing in energy efficiency projects”. On the other hand, results were found indicating that “the organizations involved in the survey had a very good awareness of additional benefits, other than energy savings, that could be applied to payback period calculations. However, the evidence obtained also demonstrated that no substantial methodology existed to be able to include the true value of all the relevant benefits in payback period calculations for energy efficiency projects” [18]. In another survey for a different sector [19], it was noted that the “companies are becoming more sophisticated in their energy management. A surprising 69% use energy efficiency as a risk management tool. Furthermore, many are willing to tolerate long-term

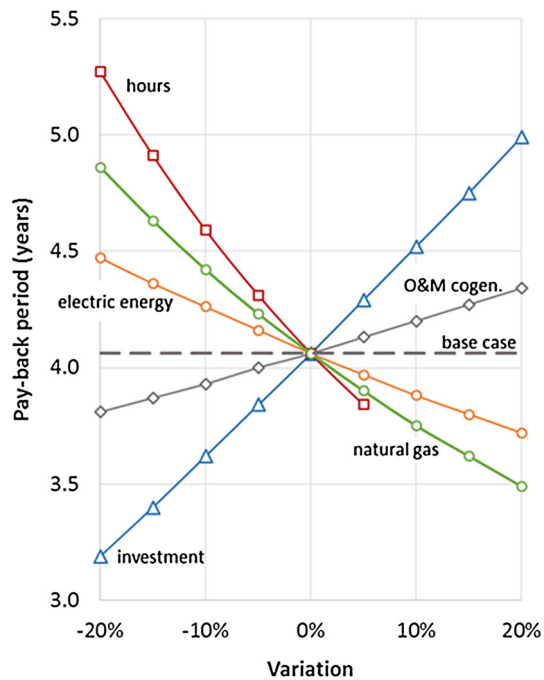
Table 9 Annual expenses with power, steam and cooling water

<i>j</i>	Expense ($\times 10^3$ USD/year)	Current situation ($i = cur$)	With cogeneration ($i = cg$)		Revenue
			Ejectors off	Ejectors on	
Power	$E_{i,p}$	21,070.378	10,301.740	10,466.732	301.896
Steam	$E_{i,st}$	1,939.135	0	1,546.455	703.248
Cooling water ^a	$E_{i,cw}$	232.380	102.364	61.923	68.093
Total		23,552.451	10,404.103	12,075.110	1,073.238

^aEvaporation ratio $r_{ev} = 1\%$

Table 10 Sensibility analysis results

Parameter	Parameter values		Payback period (base case 4.06 years)	
	Base	Varied	Varied	Variation from base case (%)
C_e (USD/MWh)	59.12	6032	3.88	− 4.38
C_{ng} (USD/m ³)	0.28	0.308	3.75	− 7.57
C_{cw} (USD/m ³)	1.00	1.10	4.04	− 0.49
$C_{om, cg}$ (USD/MWh)	15	16.5	4.20	+ 3.35
$C_{om, b}$ (USD/MWh)	5	5.5	4.01	− 1.30
H (h)	7920	8712	3.64	− 10.3
k (years)	15	16.5	4.04	− 0.49
j (%)	12	13.2	4.10	+ 0.97
b_p	0.7	0.77	3.81	− 6.15
I ($\times 10^6$ USD)	4.358	4.777	4.52	+ 11.2

**Fig. 10** Influence of the most sensible parameters on the payback period

investments to help achieve greater efficiency: one-half of respondents say that the maximum payback time for energy efficiency investments is 5 years or longer”.

5 Conclusion

In this paper, a bottoming cogeneration plant was proposed to recover heat from the dedusting system of a Brazilian mini-mill. The actual operational data were considered to calculate the heat available in the off-gas stream and to conceptualize a plant to generate power and superheated steam for the ejectors of the degassing process. Consequently, the off-gas stream would be naturally cooled down

by the cogeneration plant, contributing to the reduction in the consumption of water for off-gas cooling upstream the baghouse. To damp the off-gas transient temperature profile and assure a more stable operation of the plant, a thermal reservoir (TR) based on a mixture of two different salts was proposed and sized. Results show that the plant is technically feasible. The TR was able to provide off-gas at constant temperature for the heat recovering steam generator (HRSG). The HRSG is able to provide about half of the steam demanded by the degassing process, so that the remaining demand should be provided by the existing boilers of the mini-mill. The steam turbine operation depends on the degassing process operation and generates more power when the degassing process does not require steam. Even in this case, the power generated is small when compared with the power demand of the electric arc furnace. The consumption of cooling water, on the other hand, presented a significant reduction. From an economic point of view, the costs of the power, steam and cooling water for cogeneration are lower than the actual mini-mill current costs, resulting in a positive revenue. However, the investments required for the plant are very high, so that the revenue generated by the investment would result in a relatively long payback period. A sensibility analysis showed that the most influential parameters in the payback period are total investment, the number of operating hours, the natural gas cost, the electric energy cost and the O&M costs for cogeneration, respectively. These parameters were varied to establish both worst and best case scenarios. The payback period was found quite shorter in the best case scenario, but significantly higher in the worst case. In the best case scenario, the payback period could be accepted in the Brazilian steel industry, but it is still not short enough to be accepted in the base case. The influence of the scale of the plant, irreversibilities and cogeneration on the economic attractiveness must be further investigated, as well as alternatives that involve heat recovery only for steam

generation. However, there is a trend to accept higher payback in energy efficiency projects, since recent surveys abroad found in the literature indicate that the companies are aware of the additional benefits, other than energy savings, which could be applied to payback period calculations and many of them are willing to tolerate long-term investments to help achieve greater efficiency.

References

1. US Environmental Protection Agency (2007) Energy trends in selected manufacturing sectors: opportunities and challenges for environmentally preferable energy outcomes. http://www.techstuff.com/epa_energy.htm. Accessed Feb 2016
2. Steinparzer T, Haider M, Zauner F, Enickl G, Michele-Naussed M, Horn AC (2013) Electric arc furnace off-gas heat recovery and experience with a testing plant. *J Iron Steel Res Int* 85(4):519–526. <https://doi.org/10.1002/srin.201300228>
3. McBrien M, Serrenho AC, Allwood JM (2016) Potential for energy savings by heat recovery in an integrated steel supply chain. *Appl Therm Eng* 103:592–606. <https://doi.org/10.1016/j.applthermaleng.2016.04.099>
4. Jouhara H, Almahmoud S, Chauhan A, Delpech B, Nannou T, Tassou SA, Llera R, Lago F, Arribas JJ (2017) Experimental investigation on a flat heat pipe heat exchanger for waste heat recovery in steel industry. *Energy Procedia* 123:329–334. <https://doi.org/10.1016/j.egypro.2017.07.262>
5. Thompson S, Si M (2014) Strategic analysis of energy efficiency projects: case study of a steel mill in Manitoba. *Renew Sustain Energy Rev* 40:814–819. <https://doi.org/10.1016/j.rser.2014.07.140>
6. Tarrés J, Maas S, Scholzen F, Zürbes A (2014) Simulated and experimental results on heat recovery from hot steel beams in a cooling bed applying modified solar absorbers. *J Cleaner Product* 68:261–271. <https://doi.org/10.1016/j.jclepro.2014.01.020>
7. Chen L, Yang B, Shen X, Xie Z, Sun F (2015) Thermodynamic optimization opportunities for the recovery and utilization of residual energy and heat in China's iron and steel industry: a case study. *Appl Therm Eng* 86:151–160. <https://doi.org/10.1016/j.applthermaleng.2015.04.026>
8. Pili R, Romagnoli A, Spliethoff H, Wieland C (2017) Technoeconomic analysis of waste heat recovery with ORC from fluctuating industrial sources. *Energy Procedia* 129:503–510. <https://doi.org/10.1016/j.egypro.2017.09.170>
9. Ramirez M, Epelde M, de Arteché MG, Panizza A, Hammer-schmid A, Baresi M, Monti N (2017) Performance evaluation of an ORC unit integrated to a waste heat recovery system in a steel mill. *Energy Procedia* 129:535–542. <https://doi.org/10.1016/j.egypro.2017.09.183>
10. Nardin G, Meneghetti A, Dal Magro F, Benedetti N (2014) PCM-based energy recovery from electric arc furnaces. *Appl Energy* 136:947–955. <https://doi.org/10.1016/j.apenergy.2014.07.052>
11. Brandt C, Schuller N, Gaderer M, Kuckelkorn JM (2014) Development of a thermal oil operated waste heat exchanger within the off-gas an electric arc furnace at steel mills. *Appl Therm Eng* 66:335–345. <https://doi.org/10.1016/j.applthermaleng.2014.02.003>
12. Gaggioli W, Fabrizi F, Fontana F, Rinaldi L, Tarquini P (2014) An innovative concept of a thermal energy storage system based on a single tank configuration using stratifying molten salts as both heat storage medium and heat transfer fluid, and with an integrated steam generator. *Energy Procedia* 49:780–789. <https://doi.org/10.1016/j.egypro.2014.03.085>
13. Lora EES, Nascimento MAR (2004) Thermoelectric generation: planning, design and operation (in Portuguese), vol 1. Inter-ciência, Rio de Janeiro
14. Borgnakke C, Sonntag RE (2008) Fundamentals of thermodynamics. Wiley, New York
15. Santos CFP (2016) Thermoeconomic analysis and ecological efficiency of a thermoelectric power plant with chemical absorption of CO₂ (in Portuguese). Dissertation (Master in Mechanical Engineering). São Paulo State University (UNESP), School of Engineering, Guaratinguetá
16. Vilela IAC (2007) Development of a thermoeconomic model which takes into account the environmental impacts (in Portuguese). Thesis (Doctor in Mechanical Engineering). São Paulo State University (UNESP), School of Engineering, Guaratinguetá
17. Jacobs JA, Schneider M (2009) Cogeneration application considerations. GE Energy, GER3430G (05/09). https://www.gepower.com/content/dam/gepower-pgdp/global/en_US/documents/technical/ger/ger-3430g-cogeneration-application-considerations.pdf. Accessed 24 Aug 2017
18. OEDC Steel Committee (2015) Energy efficiency in the steel sector: why it works well, but not always. <https://www.oecd.org/sti/ind/Energy-efficiency-steel-sector-1.pdf>. Accessed 28 Aug 2017
19. Economist Intelligence Unit (2012) Energy efficiency and energy savings: a view from the building sector. The economist. http://www.bpie.eu/uploads/lib/document/attachment/16/EIU_Case_Study_Report_2012.pdf. Accessed 28 Aug 2017